Pattern Recognition 42 (2009) 523 – 530

Contents lists available at ScienceDirect

Pattern Recognition

journal homepage: www.elsevier.com/locate/pr

Membrane boundary extraction using circular multiple paths

Changming Sun[a,*], Pascal Vallotton[a], Dadong Wang[a], Jamie Lopez[b], Yvonne Ng[b], David James[b]

[a]CSIRO Mathematical and Information Sciences, Locked Bag 17, North Ryde, NSW 1670, Australia
[b]Garvan Institute of Medical Research, 384 Victoria Street, Darlinghurst, Sydney, NSW 2010, Australia

ARTICLE INFO

Article history:
Received 30 May 2008
Received in revised form 25 September 2008
Accepted 26 September 2008

Keywords:
Membrane
Membrane assay
High content analysis
Membrane segmentation
Membrane boundary extraction
Image transformation
Circular multiple paths
Closed contours

ABSTRACT

Membrane proteins represent over 50% of known drug targets. Accordingly, several widely used assays in the high content analysis area rely on quantitative measures of the translocation of proteins between intracellular organelles and the cell surface. In order to increase the sensitivity of these assays, one needs to measure the signal specifically along the membrane, requiring a precise segmentation of this compartment. Manual tracing of membrane boundary is very time-consuming and confronts us with issues of objectivity and reproducibility. In this paper, we present an approach based on a circular multiple paths technique on transformed images that enables us to segment the membrane compartment accurately and rapidly. We have presented three approaches for image transformation. The circular property of the multiple paths ensures that we are obtaining closed contours for the membrane boundary. The position of the multiple paths provides the edges of the membrane boundary. The effectiveness of our algorithm is illustrated using cells expressing epitope-tagged membrane proteins.

1. Introduction

The outer lipid bilayer of a cell mediates the exchange of polypeptides, lipids and other molecules and serves as an interface for inter-cell communication. Regulation of these exchanges through modulation of the concentration, activities, and spatial distribution of proteins and lipids within this cell compartment is, therefore, critical to normal cell function. Clusters of high-concentrated membrane proteins underlie important cellular processes, including exocytosis, endocytosis, mitosis, and cell migration. Membrane proteins may even be found in a crystalline state within the membrane. A majority of drugs available today exert their effect by targeting membrane proteins, mainly by antagonising the signalling action of soluble hormone-like ligands. Upon fixation and staining, membrane undergoes massive damages that compromise the continuity and uniformity of the membrane compartment. As a result, tracing the membrane of immunostained cells in confocal images is far from trivial.

Young and Gray used semi-automatic boundary detection techniques for identification of cells in differential interference contrast (DIC) microscope images mainly based on edge information [1]. Wu et al. introduced an iterative thresholding algorithm for the segmentation of cells from noisy images [2]. Ortiz de Solorzano et al. carried out nucleus and cell segmentation by identifying seeds and expanding the boundaries of the seeds until they reach the limits of the nuclei or cells [3]. This is similar to the snakes or active contour type of algorithms [4,5]. Alexopoulos et al. developed a method for quantifying cell size from DIC images by incorporating an edge detection algorithm and dynamic programming for edge linking [6]. Liang et al. used a dynamic programming procedure for boundary detection in ultrasonic artery images [7]. Other approaches related to membrane boundary extraction include those in Refs. [8–10]. The type of images used in these papers varies. The majority of the images contain cells with brighter intensity within the cell boundary. A gradient operation on this type of images should generate linear structure for the boundary. Some papers are directly using images showing brighter linear membrane structures. The type of images that we will be working on is of the latter type.

In this paper, we propose an approach for membrane boundary extraction using a circular multiple paths (CMP) technique. The use of the CMP technique in the neighbourhood of a cell boundary ensures that all the information within an extended region is taken into account. CMP enable us to obtain closed contours along the membrane boundary. The multiple paths are obtained through global optimisation via dynamic programming. The multiple paths also provides the edges of the membrane boundary which can be used to make measurements within the boundary region. We also provide a mechanism for the use of control points if necessary during the process of membrane boundary extraction.

The paper is organised as follows. We first describe our approach for membrane boundary extraction which includes steps such as cell centre selection, polar image transformation, and CMP extraction.

* Corresponding author. Fax: +61 2 9325 3200.
E-mail address: changming.sun@csiro.au (C. Sun).

0031-3203/$ - see front matter © 2008 Elsevier Ltd. All rights reserved.
doi:10.1016/j.patcog.2008.09.029

We then outline the individual steps of our algorithm. We demonstrate the capabilities of our membrane boundary extraction algorithm on a range of real images in the experimental result section, and then give conclusion remarks.

2. Membrane boundary extraction using CMP

In this section, we describe our algorithm for membrane boundary extraction using a CMP technique. It ensures that the boundary obtained is closed and has the maximal integrated image or gradient intensity along its paths.

2.1. Obtaining approximate cell location

We begin by obtaining an approximate position of the centre of the cell. This can be achieved interactively or through an automated process. With the interactive approach, a user can click a point close to the centre of the cell on the image. In an automated approach, the approximate centre of the cell may be obtained by the automated segmentation of the nucleus channel if available. The approximate centre position can actually be anywhere within a certain distance of the cell centre. This approximate position of the cell centre will be used next for transforming the input image or a local region of an image into polar coordinates to obtain the membrane boundary. The "+" sign in Fig. 1(a) indicates an approximate position of the cell centre. For complicated cell boundaries, two point positions within the membrane boundary may be necessary. This situation will be further discussed in the next subsection.

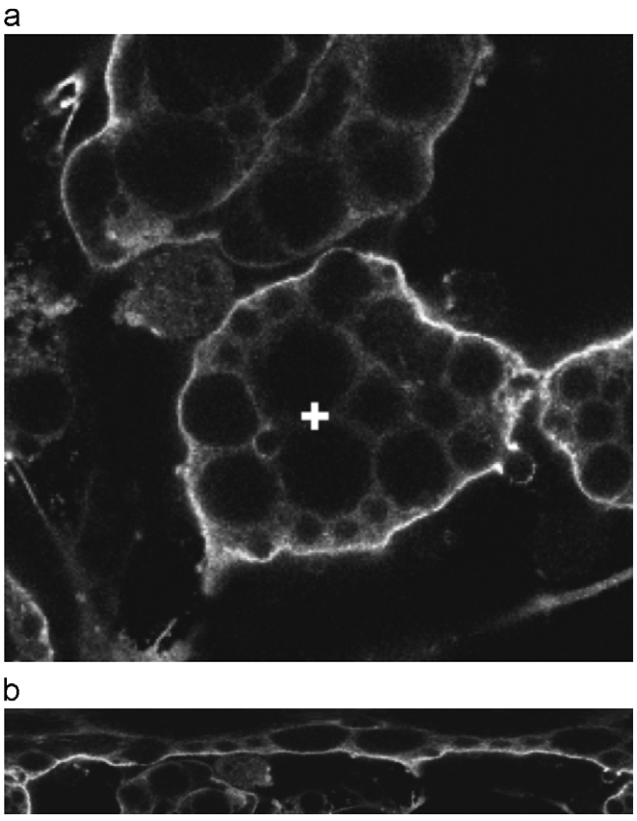

Fig. 1. Polar transformed image for a local region of an input image. (a) Input image with a cross indicating the approximate centre of cell; (b) polar transformed image.

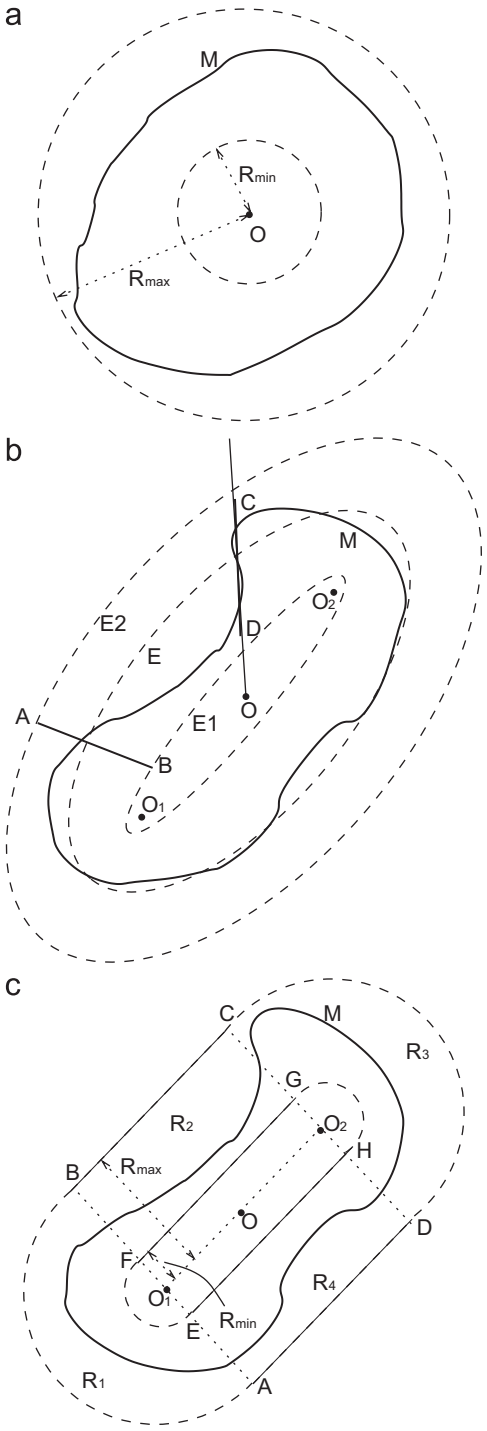

Fig. 2. Different approaches for image transformation. (a) Circular disk region or donut shaped region; (b) ellipse shaped region; (c) two half donuts and two rectangular regions.

2.2. Image transformation for boundary extraction

The neighbourhood around the approximate cell centre, a circular region as shown in Fig. 2(a), is transformed into polar coordinates for membrane boundary extraction. In the transformed image, as illustrated in Fig. 1(b), the top row corresponds to the centre point. The bottom row corresponds to the outer perimeter of the circular region with radius R_{max}. If one is able to limit the range of the radius of the membrane boundary from the cell centre, the circular region

can be restricted to a "donut" region, as bounded by the two circles with radii R_{min} and R_{max}. One set of R_{min} and R_{max} values can be selected for all the cells in the image. In this case, one needs to make sure that R_{min} is smaller than the minimum cell radius within the image and R_{max} is larger than the maximum cell radius. One can also set different R_{min} and R_{max} values for each individual cell. The membrane boundary in the transformed image appears as a bright linear object going from left to right of the image. The left and the right sides of the transformed image are neighbouring columns. That is, they are from neighbouring radial segments from the approximate cell centre of the input image. Depending on the position of this cell centre in the original image, portions of the polar transformed image may contain no values if the position of these points fall outside the original image. We can assign special values on these points in the transformed image.

For elongated shapes of the membrane boundary, we can use the shape of a "squeezed" donut, as illustrated in Fig. 2(b), bounded by the two curves E_1 and E_2, the inside and outside boundaries. Given two points O_1 and O_2, which can be treated as the foci of an ellipse, together with the length of its semi-major axis a, the shape of the ellipse E can be obtained. The half distance between O_1 and O_2 defines the linear eccentricity c of the ellipse E. From c and a, the semi-minor axis b can be obtained as $b=\sqrt{a^2-c^2}$ [11,12]. The angle of the ellipse from the horizontal x-axis, θ, can be calculated from the positions of O_1 and O_2. Based on the lengths of a, b, and the angle θ of the ellipse, the parametric function of the ellipse E can be written as

$$\begin{cases} x(t)=x_0+a\cos t\cos\theta-b\sin t\sin\theta \\ y(t)=y_0+b\sin t\cos\theta+a\cos t\sin\theta \end{cases} \quad (1)$$

where (x_0,y_0) is the centre position of the ellipse, i.e. the midpoint O of O_1 and O_2. t is the curve parameter, $-\pi\leqslant t<\pi$.

When carrying out the polar transformation, the radial segment CD still passes through the centre point O. This is similar to the case in Fig. 2(a) but with a region of a squeezed donut shape. A multiple value situation may still occur. As illustrated in Fig. 2(b), with an approximate cell centre position at O, a radial line segment OC intersects the membrane boundary M three times. This translates to three positions for boundary M to appear on one particular column in the transformed image. The existence of multiple positions of the membrane boundary on one column makes it difficult for the dynamic programming type of procedure to find the correct membrane boundary.

To reduce the possibility of multiple values occurring, one may use the tangent information at one particular point on the ellipse E. A line segment AB perpendicular to the ellipse and with the segment centre on the ellipse E sweeps through the ellipse and make a squeezed donut shape as shown in Fig. 2(b). This donut shape transforms into a rectangular image in the polar space. A line extending the segment AB does not always pass through the ellipse centre O. The unit normal vector to the tangent, i.e. along the direction of segment AB, is

$$\begin{cases} x_N(t)=\dfrac{-b\cos t\cos\theta+a\sin t\sin\theta}{\sqrt{a^2\sin^2 t+b^2\cos^2 t}} \\ y_N(t)=\dfrac{-a\sin t\cos\theta-b\cos t\sin\theta}{\sqrt{a^2\sin^2 t+b^2\cos^2 t}} \end{cases} \quad (2)$$

In complex situations as mentioned above, we can use another approach to transform the input image with two centre points within the cell to eliminate the multiple values issue as illustrated in Fig. 2(c). With two centres O_1 and O_2 within the cell boundary, we can obtain two half circles or half donuts (regions R_1 and R_3) and two rectangular regions (regions R_2 and R_4), as in Fig. 2(c). The shape of the region formed by R_1, R_2, R_3 and R_4 looks like a sport oval track. One of the half donut is obtained by swiping line segment EA clockwise to FB; the other half donut is obtained by swiping line segment GC clockwise to HD. The length of the line segment is the difference between the maximum radius R_{max} and the minimum radius R_{min} where R_{min} can be 0. The transformed images for these two half donuts R_1 and R_3 in the polar coordinate form two rectangles R'_1 and R'_3. The two rectangles for R_2 and R_4 are bounded by $FBCG$ and $HDAE$, respectively. The four rectangles, R'_1, R_2, R'_3 and R_4, are stacked together in this order to form a single rectangular image that is used for membrane boundary extraction.

The size of the transformed image depends on the angular resolution and the radius that we specify in the polar coordinate. Fig. 1 shows an example of the transformed image in a cell region of the input image. Fig. 1(a) is the input image with the small plus sign indicating the approximate position for the cell centre; and Fig. 1(b) is the local region around the cell in polar coordinates.

2.3. Obtaining circular paths

We obtain a single circular shortest path (CSP) or CMP from the polar transformed image for extracting the membrane boundary. The circular property of the paths ensures that the membrane boundary obtained is a closed contour. In the next two subsections we describe algorithms for obtaining a single shortest path and multiple paths from left to right of a rectangle image. We then describe approaches for obtaining circular paths.

2.3.1. Obtaining a single path

In some cases, one may just need to extract a single closed contour along the centre of the membrane boundary. In this case, a single CSP can be extracted. An easy approach to extract the membrane boundary is via the use of the dynamic programming technique to obtain a CSP on the transformed image. This path should go through the centre line of the membrane boundary.

The pseudocode for obtaining the shortest path from left to right in the transformed image using dynamic programming is given in the following Algorithm.

Algorithm. Shortest path via dynamic programming().
initialising cost in the first column:
for each $j\in C_1$ **do**
  $d_{1j}:=c_{1j}$
  $q_{1j}:=nil$
obtaining accumulated cost (*loop over columns*):
for $h:=2$ ***to*** v **do**
  foreach $j\in C_h$ **do**
    $d_{hj}:=c_{hj}+\min_{i\in\{|i-j|\leqslant 1\}}\{d_{h-1,i}\}$
    $q_{hj}:=\operatorname{argmin}_{i\in\{|i-j|\leqslant 1\}}\{d_{h-1,i}\}$
picking up the minimum value in the last column and backtracking
for $h:=v$ ***to*** 1 **do**
  backtrack with q_{hj} to find the path

In this pseudocode, d_{hj} is the accumulated cost for the j th point for the h th column; q_{hj} holds the backtracking information for d_{hj}; v is the number of columns; C_h is the set of pixels in column h; i is the pixel location on the previous column; j is the pixel location on the current, h th, column; and c_{hj} is the connection cost from i to j, and takes the intensity value at position (h,j) in the transformed image. The process of obtaining the accumulated cost involves the collection of the current best cost at a point and its backtracking information. Note that the dynamic programming approach for shortest path extraction takes advantage of the regular structure of the transformed image, i.e. a rectangular image. It starts with all the points on the left boundary of the transformed image; then loops through all the other columns from left to right and finishes at the right boundary. A minimum cost is selected in one of the positions in the right column, and then backtracking is carried out to find the shortest path. The dynamic programing approach is different from

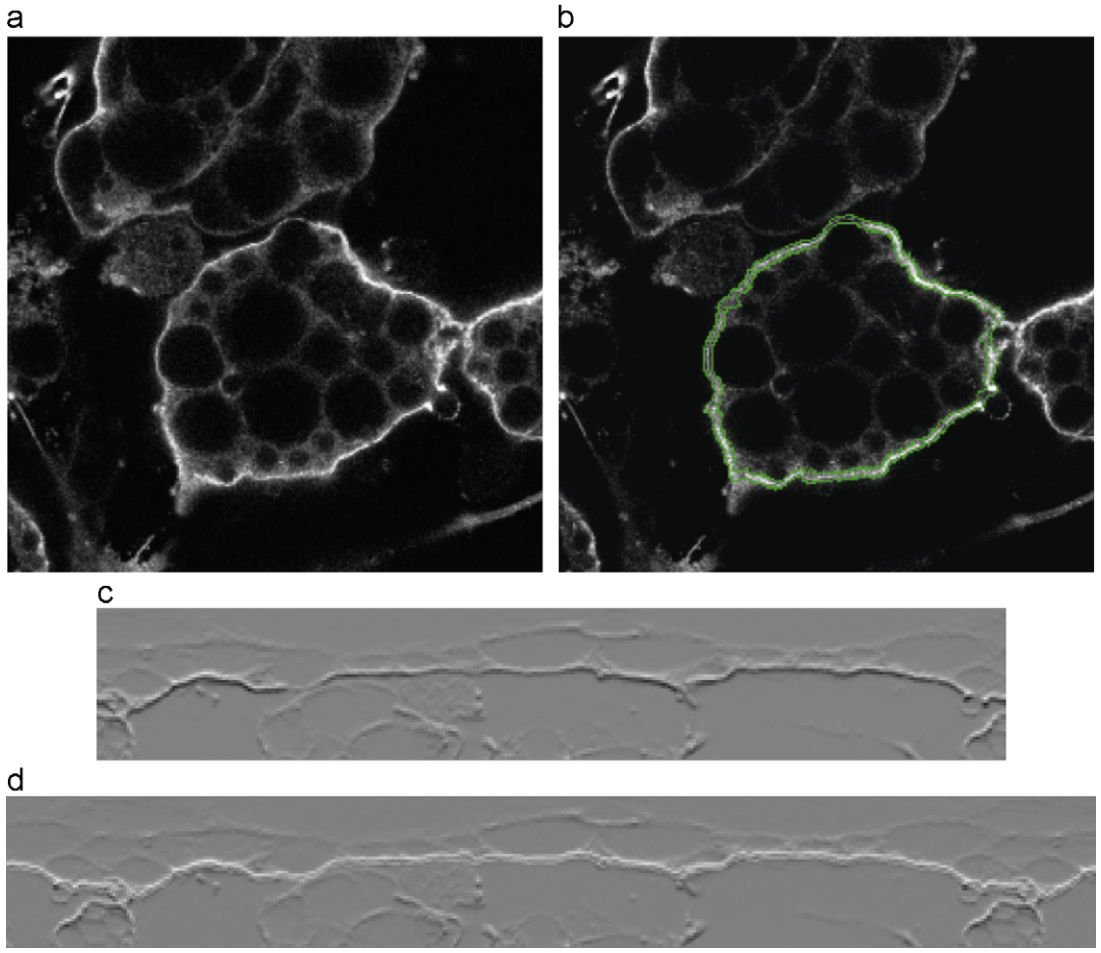

Fig. 3. Membrane boundary extraction. (a) Input image, same as Fig. 1(a), but without showing the approximate centre point; (b) membrane boundary (inside and outside) extracted and overlaid to the input image; (c) one dimensional gradient along the vertical direction in the transformed image showing the bright and dark sides of the membrane; (d) membrane boundary overlaid on the patched image. Notice the image patching at the end of (c) to become (d).

the ordinary shortest path finding in a graph structure where one needs to provide a source and a sink nodes.

2.3.2. Obtaining multiple paths

We can obtain the membrane boundary by detecting the inside and outside edges of the boundary. The inside and outside edges together form a thin band along the boundary with various thickness across it. The detection of two paths along these edges can be carried out using the multiple paths extraction method based on constrained expanded trellis (CET) as described in Ref. [13]. The gradients across the membrane boundary should have opposite signs on the inside and outside boundary. We can use the sign function when calculating the cost of paths.

The cost of each single path can be written as

$$C(P) = \sum_{h=1}^{v} c_0(h, p_h) + \sum_{h=1}^{v-1} c_1(h, p_h, p_{h+1}) \tag{3}$$

where c_0 takes the cost value from $c_{h,j}$ given in Section 2.3.1. p_h is the path position on column h. For multiple paths extraction, we use gradient information of the transformed image as input. c_1 is a first order cost function relating the shape of the path at the current location. The cost of the multipath $\vec{P}$ is the sum of the costs of the K component paths:

$$C(\vec{P}) = \sum_{k=1}^{K} C(P^k)$$

From this we may derive the cost functions for the multiple paths $\vec{P}$ from the sums of the cost functions of each individual path k:

$$C(\vec{P}) = \sum_{k=1}^{K} \sum_{h=1}^{v} c_0(h, p_h^k) + \sum_{k=1}^{K} \sum_{h=1}^{v-1} c_1(h, p_h^k, p_{h+1}^k) \tag{4}$$

where p_h^k is the position of the k th path on column h. We use the CET method for extracting multiple paths, simultaneously in the transformed image. In the current implementation,

$$c_1(h, p_h^k, p_{h+1}^k) = \begin{cases} 0 & \text{if } |p_h^k - p_{h+1}^k| \leqslant 1 \\ \infty & \text{otherwise} \end{cases}$$

2.3.3. Ensuring closed contour

Sun and Pallottino developed several algorithms for a single CSP extraction on regular grids or images [14]. The algorithms use an efficient dynamic programming approach and ensure that the shortest path obtained is circular. These algorithms are the Multiple Search Algorithm (MSA), Image Patching Algorithm (IPA), Multiple Backtracking Algorithm (MBTA), a combination algorithm of IPA and MBTA, and an approximate algorithm. We will use the IPA algorithm here for membrane boundary extraction because it is conceptually easy to understand and is very fast. The basic idea behind IPA is to carry out image patching, a step which ensures path closure, and use a dynamic programming algorithm to find a path in the patched image.

The patching for the IPA algorithm is carried out in the horizontal direction on the left and the right sides of the transformed image.

The values of the patched regions come from the transformed image itself. A shortest path is obtained from this patched image, and a CSP may be extracted from the patched image. For detailed description of the IPA algorithm please see Ref. [14]. The algorithm given in Ref. [14] is for obtaining a single CSP in an image. We will use the same IPA algorithm for obtaining CMP simultaneously.

The steps of the IPA algorithm for CSP and CMP extraction in the transformed image are:

(1) Patch the transformed image on the left and the right sides with portions of the transformed image itself to obtain a patched image.
(2) Perform ordinary shortest path extraction using dynamic programming or multiple paths extraction on the patched image.
(3) Extract the shortest paths which lies inside the original transformed image.

2.4. Use of control points

Due to noise and the presence of other cells nearby, the extracted membrane boundary may not be optimal. Part of the boundary may shift to the boundary of other cells due to the fact that the strength of the boundary of the other cells nearby is much stronger than the cell of interest. In this case, we can add one or more control points close to the membrane boundary of interest to enforce the extracted boundary to be close to these control points. We carry out this by assigning special (e.g. large negative) values for some columns of the transformed image except for the pixels that are close to the control points. The use of control points is only necessary in difficult situations.

2.5. Membrane measurements

The measurements along the membrane boundary include total area, integrated intensity, average intensity, maximum intensity, standard deviation of intensity, and length of boundary.

For a method using a single CSP, only one path along the centre line of the membrane boundary is obtained. To make measurements along the boundary, a fixed width across the boundary can be used. The results of CMP contain multiple paths along the edges of the membrane boundary, as shown in Fig. 3(b). One of the paths is along the inside edge of the centre line, while the other path is along the outside edge of the centre line. The region between the two paths from CMP can be used for membrane measurements.

3. Membrane boundary extraction algorithm

We outline here the main steps of our algorithm for obtaining membrane boundary from images using our CMP technique. The summary steps are:

(1) Locate the approximate centre of the cell. This can be interactive or automated. For elongated cells, two point positions can be used.
(2) Add extra control points close to the membrane boundary if necessary.
(3) Transform the input image in a local region of the cell from Cartesian to polar coordinate system.
(4) Carry out gradient operation if needed for the multiple paths cases.
(5) Apply circular single or multiple paths extraction algorithm to the transformed image.
(6) Convert the paths obtained back to the original image space.
(7) Measure the required information along the membrane boundary.

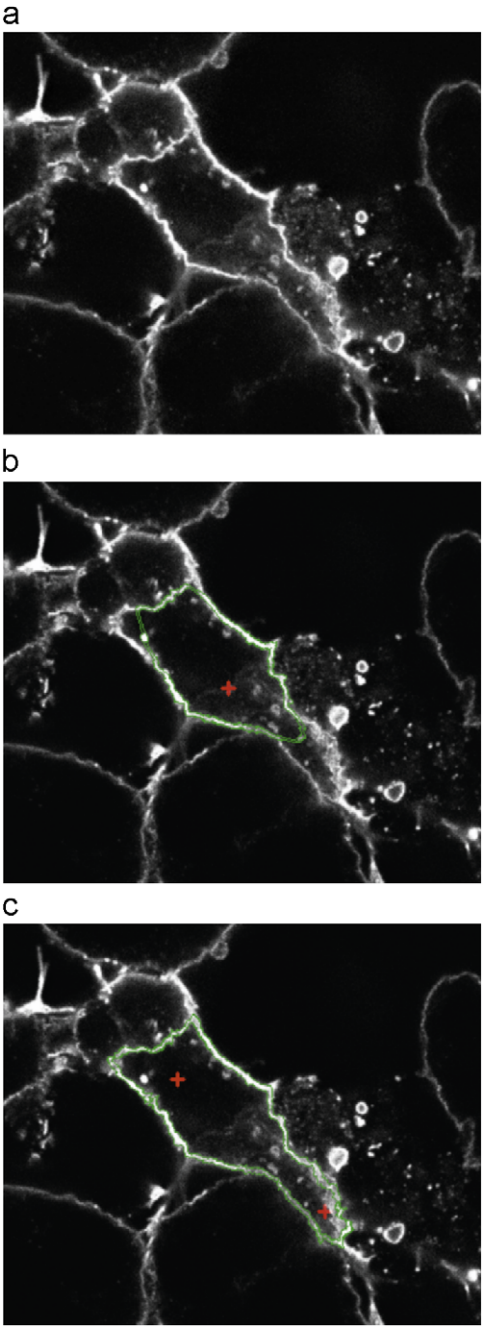

Fig. 4. The effect of one or two centre points (as shown with the "+" signs) when carrying out image transformations with complex membrane boundary shapes. (a) Input image; (b) membrane boundary obtained with a single cell centre; (c) membrane boundary obtained with two cell centres.

4. Experimental results

In this section we present results obtained from images of adipocytes expressing epitope-tagged membrane proteins using our membrane boundary extraction algorithm.

Fig. 3(a) shows an image of a cell; and its membrane boundary, obtained using our algorithm, is shown in Fig. 3(b). Fig. 3(a) is the input image. The two contours in Fig. 3(b) shows the inside and outside membrane boundary. Fig. 3(c) is the gradient of the transformed image. Fig. 3(d) is the patched image of Fig. 3(c) with the boundary overlaid.

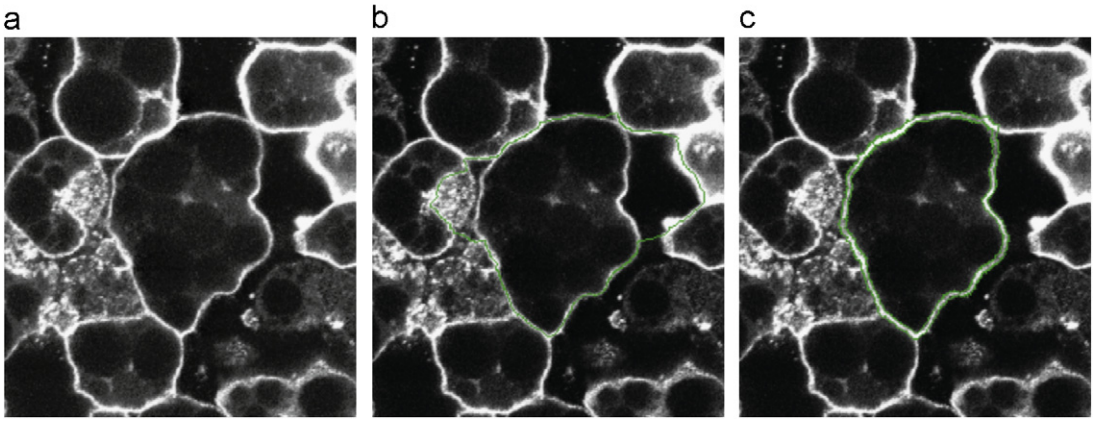

Fig. 5. Membrane boundary extraction with a single path along the centre and two paths along the inside and outside edges. (a) Input image; (b) result with a single path extracted along the membrane centre line using just image intensity information; (c) result with two paths along the inside and outside edges using gradient information.

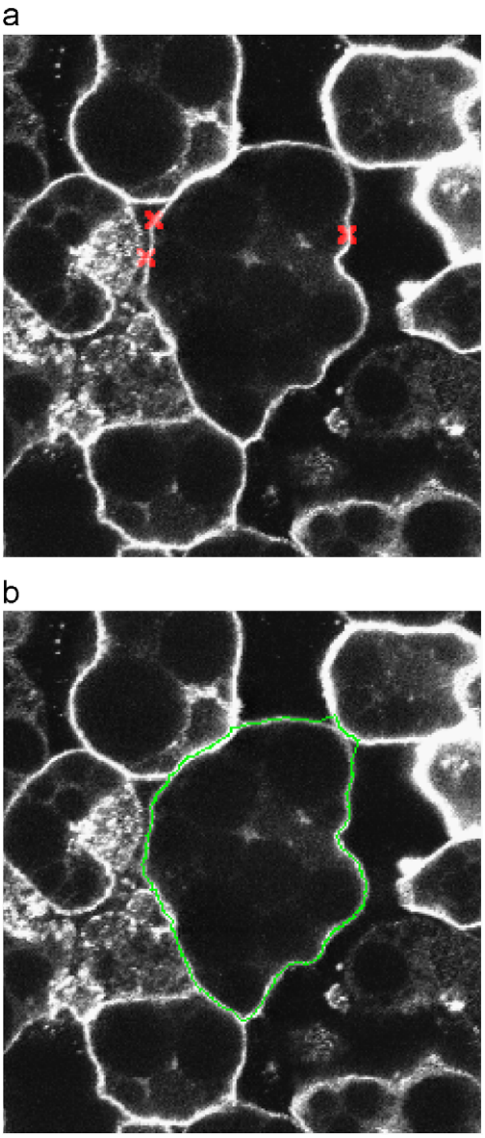

Fig. 6. Membrane boundary extraction with control points to correct the path obtained in Fig. 5(b). (a) Three control points shown with the "×" signs; (b) results with the use of the three control points.

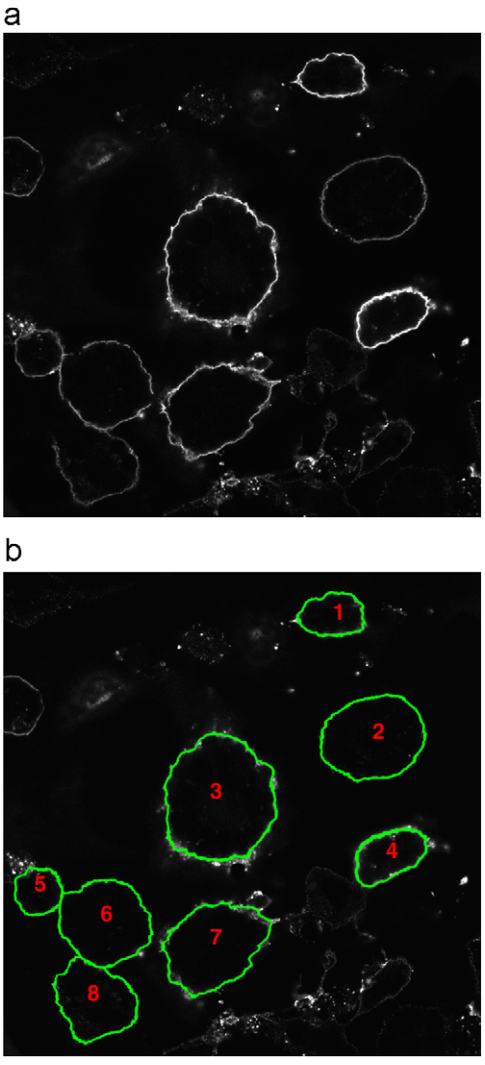

Fig. 7. More examples for membrane extraction. (a) Input image; (b) eight membrane boundaries extracted and overlaid on the input image.

Fig. 4 shows the effect of using one or two centre points when carrying out image transformations with complex membrane boundary shapes. The centre points used are shown with the "+" signs in

Table 1
Example measurements on membrane boundaries as shown in Fig. 7(b).

Membrane no.	Area	Max. int.	Mean int.	Integrated int.	Std. dev. int.
1	1982	255	150.16	297 611	63.39
2	3416	255	62.94	215 008	35.12
3	4491	255	152.39	684 367	57.10
4	2585	255	192.53	497 691	59.73
5	1780	255	73.74	131 254	40.64
6	3257	236	70.51	229 638	42.30
7	3470	255	117.95	409 291	53.26
8	3010	222	46.36	139 541	30.97

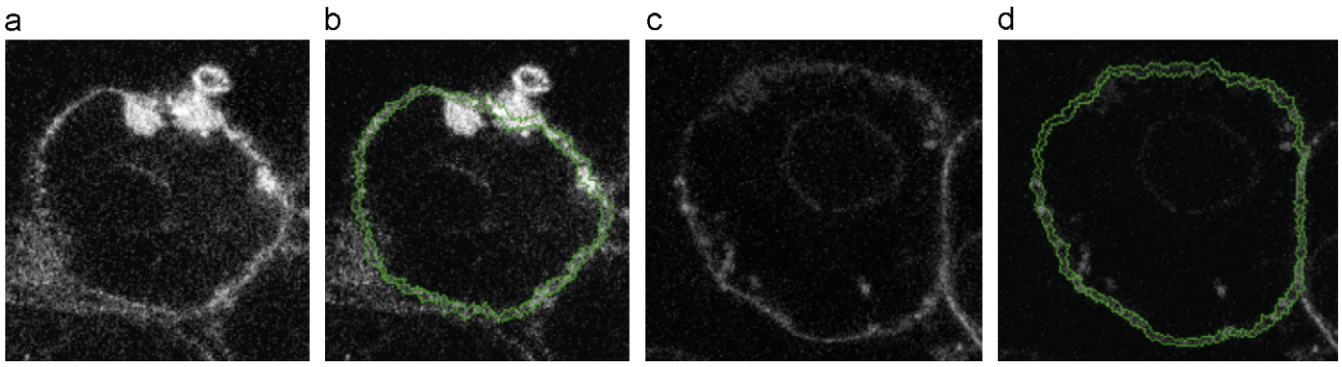

Fig. 8. More examples of membrane extraction on cells in noisy images. (a, c) Subimages of the input images; (b, d) results of our CMP algorithm on (a, c), respectively.

the image. Fig. 4(a) is the input image with membrane boundary of complex shape. Fig. 4(b) shows the membrane boundary obtained with a single cell centre; and Fig. 4(c) shows the membrane boundary obtained with two cell centres.

Fig. 5 shows the results for membrane boundary extraction using a single path and two paths. The single path is obtained using single CSP technique based on image intensity information. The two paths are obtained using the CMP technique based on image gradient information. It can be seen clearly that the CMP method is much more robust compared with the single path method. Fig. 5(a) is the input image. Fig. 5(b) shows the boundary obtained with errors. Fig. 5(c) gives the correct inside and outside membrane boundary.

Fig. 6 shows the use of control points to regulate the shape of the CSP path. Fig. 5(b) is the result without the use of control points. The membrane boundary obtained is far from the desired boundary. Fig. 6(a) shows three control points with the "×" signs. Fig. 6(b) shows the membrane boundary obtained using the three control points. This boundary is very close to the true membrane boundary.

Fig. 7 shows more examples of membrane boundary extraction using the CMP method. Fig. 7(b) shows eight membrane boundaries extracted from the input image shown in Fig. 7(a). Table 1 gives some example measurements, such as area, maximum intensity, mean intensity, integrated intensity, and standard deviation of intensity, on the eight membrane boundaries shown in Fig. 7(b). Fig. 8 gives more examples of our membrane boundary extraction method with cells in noisy images without using control points.

We have also tested the effect of changing the centre of the cell on the extraction of membrane boundary. It turns out that the position of the cell centre can be very flexible within the cell. As long as the approximate centre is not too close to the membrane boundary and there is no boundary folding for a particular viewing direction from the centre or, in complicated cases, from the two centres, our algorithm is able to find the correct boundary. For the majority of membrane boundaries, a single centre position is enough to transform the image in a circular or donut region without the side-effect of boundary folding or the appearance of multiple values in the transformed image. For complicated shapes of membrane boundary, the transformation using two points as shown in Figs. 2(b, c) is needed.

The running time of our algorithm was tested on an Intel Pentium 4 with a 2.66 GHz CPU under the Linux operating system. Our images were 8 bit/pixel. For colour images, only the intensity information or a single channel was used. For a 512×512 pixel image, analysis takes about 0.03 s CPU time for the single CSP method and about 0.4 s CPU time for the CMP method for one membrane boundary extraction. The algorithm described in Ref. [13] for multiple paths extraction use a multiway trie data structure. This requires the conversion of floating point gradient data to the range of [0–255]. An implementation of the method in Ref. [15] can use floating points data. But the algorithm is much slower.

The use of CMP technique for membrane boundary extraction ensures that the boundary obtained for a cell is a closed contour. The global optimisation property of the shortest path technique via the use of dynamic programming delivers the global minima or maxima along the membrane boundary. Because it is a global optimisation approach, small gaps in a local region can be filled and hence generate a continuous boundary. The fact that we are obtaining two paths at the same time along the inside and outside of the membrane boundary using the gradient information with opposite signs makes our algorithm very robust compared with a single path method just using intensity or gradient magnitude information. In contrast, techniques using snakes, level-sets, or watershed may sometimes stop at local minima, depending on initialisation. The two paths obtained along the inside and outside boundaries also provide the region for membrane measurement. If only one path is obtained along the centre line of the membrane, a region with fixed width along the membrane may need to be used for measurements.

5. Conclusions

We have introduced a new capability for measuring fluorescence signals precisely within the plasma membrane compartment. In our

method, the membrane corresponds to an optimal trace with highest integrated intensity or two traces with highest gradient values along the inside and outside membrane boundary. The boundaries are obtained through the use of our circular single or multiple paths technique that ensures a closed contour with maximum intensity or gradient values along the membrane boundary. The circular multiple paths are obtained on the polar transformed images. The effectiveness of our algorithm has been illustrated using many real images. We are planning to make available the functionalities developed in this paper in HCA-Vision, our cell analysis software.

Acknowledgement

We thank Dr Rongxin Li of CSIRO for his comments on an early draft of this paper. A preliminary version of this paper was presented in a conference [16].

References

[1] D. Young, A.J. Gray, Semi-automatic boundary detection for identification of cells in DIC microscope images, in: Sixth International Conference on Image Processing and its Applications, vol. 1, Dublin, Ireland, 14–17 July, 1997, pp. 346–350.
[2] H.-S. Wu, J. Barba, J. Gil, Iterative thresholding for segmentation of cells from noisy images, J. Microsc. 197 (3) (2000) 296–304.
[3] C. Ortiz De Solorzano, R. Malladi, S.A. Lelièvre, S.J. Lockett, Segmentation of nuclei and cells using membrane related protein markers, J. Microsc. 201 (3) (2001) 404–415.
[4] M. Kass, A. Witkin, D. Terzopoulos, Snakes: active contour models, Int. J. Comput. Vision 1 (4) (1988) 321–331.
[5] D.J. Williams, M. Shah, A fast algorithm for active contours and curvature estimation, CVGIP: Image Understanding 55 (1) (1992) 14–26.
[6] L.G. Alexopoulos, G.R. Erickson, F. Guilak, A method for quantifying cell size from differential interference contrast images: validation and application to osmotically stressed chondrocytes, J. Microsc. 205 (2) (2002) 125–135.
[7] Q. Liang, I. Wendelhag, J. Wikstrand, T. Gustavsson, A multiscale dynamic programming procedure for boundary detection in ultrasonic artery images, IEEE Trans. Medical Imaging 19 (2) (2000) 127–142.
[8] S. Raman, C.A. Maxwell, M.H. Barcellos-Hoff, B. Parvin, Geometric approach to segmentation and protein localization in cell culture assays, J. Microsc. 225 (1) (2007) 22–30.
[9] H. Chang, K.L. Andarawewa, J. Han, M.H. Barcellos-Hoff, B. Parvin, Perceptual grouping of membrane signals in cell-based assays, in: Fourth IEEE International Symposium on Biomedical Imaging: From Nano to Macro, 12–15 April, 2007, pp. 532–535.
[10] N.L. Prigozhina, L. Zhong, E.A. Hunter, I. Mikić, S. Callaway, D.R. Roop, M.A. Mancini, D.A. Zacharias, J.H. Price, P.M. McDonough, Plasma membrane assays and three-compartment image cytometry for high content screening, ASSAY Drug Dev. Technologies 5 (1) (2007) 29–48.
[11] Ellipse. ⟨http://mathworld.wolfram.com/Ellipse.html⟩.
[12] Eccentricity (Mathematics). ⟨http://en.wikipedia.org/wiki/Eccentricity_(mathematics)⟩.
[13] C. Sun, B. Appleton, Multiple paths extraction in images using a constrained expanded trellis, IEEE Trans. Pattern Anal. Mach. Intell. 27 (12) (2005) 1923–1933.
[14] C. Sun, S. Pallottino, Circular shortest path in images, Pattern Recognition 36 (3) (2003) 711–721.
[15] J.K. Wolf, A.M. Viterbi, G.S. Dixon, Finding the best set of K paths through a trellis with application to multitarget tracking, IEEE Trans. Aerosp. Electron. Syst. 25 (2) (1989) 287–296.
[16] C. Sun, P. Vallotton, D. Wang, J. Lopez, Y. Ng, D. James, Membrane boundary extraction using a circular shortest path technique, in: Tuan D. Pham, Xiaobo Zhou (Eds.), Proceedings of International Symposium on Computational Models for Life Sciences, Gold Coast, Queensland, Australia, December 2007, pp. 41–47.

About the Author—CHANGMING SUN received his Ph.D. from Imperial College London in 1992. Then he joined CSIRO Mathematical and Information Sciences, Australia where he is currently a Principal Research Scientist. His research interests include computer vision, image analysis, and pattern recognition. He has served on the program/organising committees of various international conferences. Dr. Sun is a member of the Australian Pattern Recognition Society.

About the Author—PASCAL VALLOTTON leads the Biotech Imaging group of CSIRO, where he and his colleagues develop new technologies for biological imaging.

About the Author—DADONG WANG received his Bachelor, Master and Ph.D. in the areas of artificial intelligence and its engineering applications. Prior to joining CSIRO, he worked in industry for six years. He joined CSIRO in 2005 as a senior software engineer driving the development of the high content analysis software, HCA-Vision.

About the Author—JAMIE LOPEZ received his Bachelor of Science with Honours from the University of Technology, Sydney and his Ph.D. from the University of NSW and the Garvan Institute of Medical Research in 2007 where he studied the cell biology of Type II Diabetes. His research focus's on mechanisms of intracellular vesicle trafficking.

About the Author—YVONNE NG received her Bachelor of Science with Honours from University of New South Wales in 2005. She is currently pursuing her Ph.D. at the Garvan Institute of Medical Research. Her research interest is in the area of molecular and cell biology of insulin action.

About the Author—DAVID JAMES is head of the Diabetes and Obesity Program at the Garvan Institute of Medical Research in Sydney. His research aims to understand the physiological effects of insulin. He is a member of the Australian Academy of Science and holds a Professor appointment through the University of NSW.